PHYSICAL REVIEW A VOLUME 43, NUMBER 11 1 JUNE 1991

Collision-induced emission in the fundamental vibration-rotation band of H_2

G. E. Caledonia and R. H. Krech
Physical Sciences Inc., Andover, Massachusetts 01810

T. D. Wilkerson
Institute of Physical Science and Technology, University of Maryland, College Park, Maryland 20742

R. L. Taylor
CVD Inc., Woburn, Massachusetts 08101

G. Birnbaum
National Institute of Standards and Technology, Gaithersburg, Maryland 20899
(Received 1 November 1990)

Measurements of collision-induced emission in the fundamental vibration-rotation band of hydrogen are presented for argon, xenon, and neon collision partners. These absolute, spectrally resolved infrared measurements were performed at high densities behind reflected shock waves over the temperature range of 900–3400 K. The emission was found to be dominated by Q-branch transitions at high temperature due primarily to the dipole moment induced by the overlap between the electron clouds of the collision pair. The strength of this interaction was evaluated from the data and compared with similar evaluations determined from low-temperature absorption studies.

I. INTRODUCTION

This paper reports studies of the collision-induced emission (CIE) in the fundamental vibration-rotation band of the hydrogen molecule. The spectrally resolved infrared emission of the H_2 band was measured at elevated temperatures and pressures using a high-density, moderate-temperature shock tube as the controlled light source. The measurements were performed for several rare-gas collision partners and were interpreted within the framework of existing theory.

Collision induction in hydrogen has been well characterized in absorption at temperatures below 400 K,[1,2] but has only recently[3,4] been studied at higher temperatures in emission. Collision-induced processes give rise to vibrational, rotational, and translational absorption and emission in molecules which by virtue of their symmetry do not have an electric dipole moment in their electronic ground state. The proximity of a collision partner makes possible the induction of a transient dipole in the colliding pair resulting from interactions due predominantly to the permanent quadrupole moment of H_2 and to the overlap of the molecular electron clouds. Such interactions produce relatively weak radiation signatures which, however, can be significant at high pressures. Indeed, CIE by H_2 has been found to be an important source of infrared radiation in planetary atmospheres,[5–7] and its inverse process, collision-induced absorption, is the dominant source of infrared opacity in stellar atmospheres.[8]

The present study focused on the high-temperature band strength and spectral shape of the H_2 fundamental vibration-rotation band centered at 2.4 μm. The band emission was measured behind reflected shocks over the temperature range of 900–3400 K. Gas mixtures of H_2 with Ne, Ar, and Xe were investigated. Since the emission is collision induced, its intensity scales as the square of the density; measurements were performed over the density range of 10–50 amagats.

A description of the experimental apparatus and techniques is provided in Sec. II. A brief review of the theory of Van Kranendonk,[9,10] and how it was applied to the present data, is presented in Sec. III. The data are summarized in Sec. IV and analyzed to evaluate the induced dipole parameters. The summary and conclusions of the study are given in Sec. V.

II. EXPERIMENTAL APPARATUS AND PROCEDURES

The measurements were performed in the Physical Sciences Inc. (PSI) shock tube facility. The shock tube is a valuable tool for this type of study because it can readily heat and equilibrate a large volume of gas at steady chemical and thermal conditions. Furthermore, the thermodynamic properties of the gas can be calculated accurately from measurements of the initial gas pressure and shock velocity. On the negative side, a measurement must be performed during a relatively short test time ($\lesssim 1.5$ ms) and thus there is little opportunity for time averaging the signal.

The emission measurements were performed behind reflected shocks in a polished stainless steel shock tube with an interior diameter of $6\frac{3}{8}$ in. The driver and test sections were 9 and 18 ft long, respectively, with $\frac{5}{8}$-in.-thick walls. A schematic diagram of the apparatus is shown in Fig. 1. The optical measurements were made

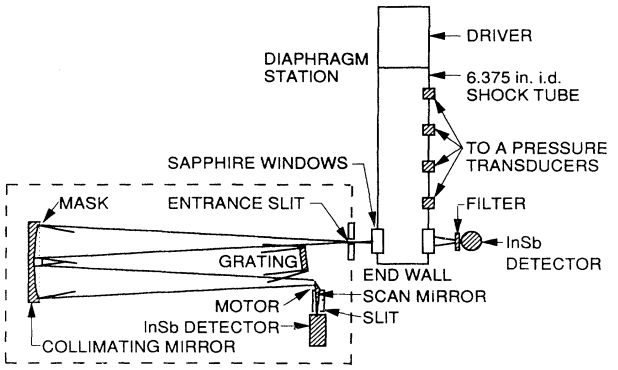

FIG. 1. Schematic of shock tube and ir instrumentation.

through 1-in.-diam×0.25-in.-thick sapphire windows located 2 in. from the end wall. Shock pressures were measured by four piezoelectric transducers located at 20-in. intervals along the test section. The shock velocity was determined from the time of arrival of the shock wave at successive stations. One pressure transducer was located at the optical port to allow a direct correlation of the emission signals with the pressure.

The test gases were ultra-high-purity grade gases supplied by Linde (use of commercial names is only for purposes of equipment identification), and were taken directly from the cylinders without further purification. The shock tube was evacuated to 10^{-8} atm by a 4-in. diffusion pump before filling, and the fill pressure was measured with a Validyne variable reluctance pressure transducer with a 0.5% accuracy. Care was taken to ensure gas purity because the strong 2.7-μm water vapor band falls within the spectral region of observation. These measures were successful since no evidence of water vapor radiation was observed in test runs in pure argon gas.

The infrared emission was monitored by two optical detection systems that were positioned 5 cm from the shock tube end wall and viewed the gas perpendicular to the shock tube axis. The total CIE band emission was monitored by a narrow band radiometer with a spectral range of 2.1–2.7 μm. CIE band spectra were obtained using a 0.5-m $f/9.1$ Ebert synchronized high-speed scanning spectrometer.[11] The instrument was originally designed in the early 1960s for high-temperature plasma studies and can scan 0.6 μm in the infrared in 30 μs. The spectrometer is synchronized to the shock front by a trigger pulse from one of the piezoelectric transducers, and has an internal wavelength calibration which allows correction for any nonuniformities in scan rate. For the present experiments, the instrument was scanned at $\sim$0.002 μm/μs with a resolution of 0.1 μm. Indium antimonide detectors (2.5×5 mm) were fabricated for the spectrometer by Infrared Industries.

The field of view of both detector systems was minimized to reduce contributions from scattered light. A 6-in. focal length telescope was added to the spectrometer to image the slit into the center of the shock tube. An aperture was placed in front of the radiometer to similarly restrict its field of view.

All instrumentation was interfaced with a computer-controlled CAMAC data acquisition system containing two ten-bit, four-channel LeCroy digitizers. The calibrations and the raw spectrum, reported as intensity versus time, were first stored in the computer and then converted into plots of either intensity or emissivity versus wavelength. The details of the data reduction procedure have been provided elsewhere.[12]

Because we deduced the fundamental CIE H_2 band strengths from spectrally resolved emission measurements, careful absolute calibration was crucial for experimental success. The absolute calibration was accomplished using standard techniques with a blackbody source. As a check, spectrally resolved emission measurements of the first CO overtone band at 4260 cm^{-1} were performed. Although the band strength of this radiation has never been measured in the temperature range of 1000–3000 K, its dipole moment has been well characterized. The details of the CO measurements were presented earlier.[13] A typical radiance measurement of the CO first overtone band is shown in Fig. 2. Background signals of $\sim$10% of the total radiance were observed. These were typical and were also seen in pure Ar that is shock heated. The source of this background radiation was not identified.

A calculated spectrum of CO is shown for comparison with the experimental spectrum. The former was obtained by a line-by-line calculation and then convolved with a triangular slit function, with a full width at half maximum (FWHM) of 0.1 μm, characteristic of the spectrometer. Note that the zero value of the calculated spectrum is set at the average level of the background intensity. The comparison between data and theory is quite good demonstrating both the lack of competing bands in

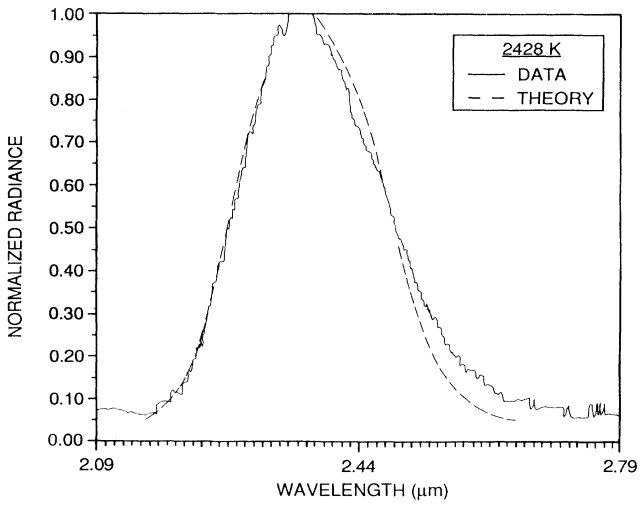

FIG. 2. CO first overtone emission $T=2458$ K. Measurement performed in reflected shock, $\rho=7.6$ amagat.

our measurements at 2.4 μm and the ability of the scanning monochromator to provide a high fidelity replication of the band emission.

Absolute CO overtone band strengths were evaluated from such data for temperatures varying between 1170 and 2600 K. Comparisons with predicted band strengths based upon transition matrix elements calculated by Chackerian and Tipping[14] were found to be quite good.[13] An estimated uncertainty of 30% in these measurements resulted in large part from run-to-run variability and background subtraction.

For the CIE measurements, the wideband radiometer was also absolutely calibrated as a cross check on the spectrometer calibration. Typically, radiometer traces exhibited a reflected shock jump, followed by a slow increase which leveled off within 0.5 ms. This increase in radiation level was correlated with radiation that was emitted downstream of the observation window and reflected by the shock tube walls.[13] The spectrometer data were corrected for this spurious additional signal arising from scattered light. The correction factor varied between 1.1 and 1.45, the value of 1.35 being typical.

Uniform test times (as defined by the pressure trace) of greater than 1 ms behind the reflected shock were routinely achieved. Measured shock pressures were always within a few percent of the pressures calculated from the Rankine-Hugoniot conservation equations using the measured incident shock velocity.[15] This velocity was typically measured with an accuracy of 1%; the corresponding temperature uncertainty was ± 50 K.

III. H_2 COLLISION-INDUCED EMISSION THEORY

The Van Kranendonk model[9] is employed here to estimate the band strength of the H_2 CIE spectrum. This theoretical treatment describes the transient dipole induced by collisions in terms of a long-range component due to quadrupolar induction and a short-range component resulting from charge deformation caused by electron overlap forces. This is the "exp-4" model, which combines an angle-independent short-range exponential term and a long-range angular dependent $1/R^4$ term due to quadrupolar induction. We note that by definition the band emissivity and absorptivity are identical.

Within this framework, the expression for the binary absorption coefficient of the fundamental band is

$$\tilde{\alpha}_1 = \lambda^2 I\tilde{\gamma} + (\mu_1^2+\mu_2^2)\tilde{J}\tilde{\gamma} = \int_0^\infty \frac{\alpha(\nu)}{\nu} d\nu \tag{1}$$

where $\tilde{\alpha}_1$ is in $\text{cm}^{-1}\,\text{amagat}^{-2}$, ν is the wave number, and $\alpha(\nu)$ is the absorption coefficient in $\text{cm}^{-1}\,\text{amagat}^{-2}$. The quantity λ in Eq. (1) is defined by

$$\lambda = (\xi/e)e^{-\sigma/\rho} \tag{2}$$

where ξ is the strength and ρ is the range of the overlap-induced dipole, and σ is the Lennard-Jones molecular diameter. The quantities μ_1 and μ_2 are amplitude parameters of the quadrupole-induced contribution, see Ref. 1, Eqs. (2.19) and (2.20) or Ref. 9, Eqs. (19) and (22), for details, and $\tilde{\gamma}$ is defined by

$$\tilde{\gamma} = \pi e^2\sigma^3/3m_0\nu_0 \tag{3}$$

where e is the electronic change, m_0 is the reduced mass of the collision pair, and ν_0 is the vibration frequency.

The quantities I and $\tilde{J}$ are radial integrals for overlap and quadrupole forces, respectively,

$$I = 4\pi\int_0^\infty e^{-2(x-1)\sigma/\rho} g_0(x)x^2 dx\ , \tag{4}$$

$$\tilde{J} = 12\pi\int_0^\infty x^{-8} g_0(x)x^2 dx\ , \tag{5}$$

where

$$g_0 = \exp[-V^*(x)/T^*]\ . \tag{6}$$

At high temperatures, quantum effects in the translation motion of the molecules can be neglected, and the classical expression for $g_0(x)$ can be used. The Lennard-Jones potential was used in $V^*(x)$. The normalized quantities are $V^* = V/\varepsilon$, $x = R/\sigma$, and $T^* = kT/\varepsilon$.

We note that there are much more sophisticated interaction potentials available for hydrogen–rare-gas complexes (for example, Refs. 16 and 17) and that the potential energy is a function of the vibrational state (see, for example, Ref. 18). Nonetheless, we adopted the simpler isotropic ground vibrational-state Lennard-Jones potential which has been used to analyze much of the earlier data. We used early estimates[9,19] of the Lennard-Jones parameters ε and σ in our analysis to allow easy comparison with the older experiments. The values used are listed in Table I. More modern potentials give significantly different values. For example, the isotropic portion of the H_2-Ar potential in Ref. 17 gives $\varepsilon = 75.2$ K and $\sigma = 3.56$ Å, significantly different from the values listed in Table I. However, as shown below, we evaluate the induced dipole parameters as functions of ε and σ and thus our analysis can be adapted to other choices of Lennard-Jones parameters.

Since the constants in the quadrupolar contribution are known, this contribution of the exp-4 model to the CIE band strength was readily evaluated. (The constants are the derivatives of the quadrupole moment and polarizability with respect to internuclear distances, and the quadrupole moment and polarizability themselves.) In one application of the model,[9] the predicted quadrupolar contribution was subtracted from the measured room-temperature band strength resulting in a measured value of the quantity $\lambda^2 I\tilde{\gamma}$. A value was then assumed for ρ and the quantity ξ was evaluated. In another analysis,[20–22] the markedly different temperature dependencies of the quadrupolar and overlap contributions were exploited. Specifically, collision-induced absorption measurements taken over the temperature range of 77–300 K were analyzed to simultaneously specify both ξ and ρ. In the present work the high-temperature emission measurements were used in conjunction with room-temperature data to evaluate both ξ (more properly, λ^2) and ρ. The theory is thus tested over a full order of magnitude in temperature.

The analysis of the spectral shape of the band employed here provides an additional discrimination between the quadrupolar and overlap contributions. The quadrupolar emissions obey Raman selection rules allow-

TABLE I. H_2–rare-gas CIE molecular parameters as described in Eqs. (1)–(3).

Gas	ρ/σ	Quadrupole $\overline{\gamma}\mu^2$ (amagat^{-2} cm^{-1})	Overlap $\overline{\gamma}\lambda^2$ (amagat^{-2} cm^{-1})	ε/K (K)	σ (Å)
He	0.088(1)	1.5×10^{-9}	5.0×10^{-8}(11)	19.4	2.74
Ne	0.102(11)	3.2×10^{-9}	1.0×10^{-7}(11)	36.2	2.85
Ar	0.08[a]	3.3×10^{-8}	1.3×10^{-7}	66.6	3.17
Xe	0.14[a]	1.1×10^{-7}	5.4×10^{-7}	90.4	3.51

[a]This work.

ing Q-, O-, and S-band transitions, i.e., $\Delta J=0,-2,+2$, respectively, while the overlap term only produces Q-band spectra. A simple model of the expected temperature-dependent spectra for the two contributions was used to analyze the data. The model incorporates transitions in all three bands for all J and employs a modified harmonic oscillator approximation to include hot band transitions (vibrational level >1) which are important at the elevated temperatures of the present measurements. (For example, at $T=3000$ K, 25% of the radiation arises from vibrational levels higher than $v=1$.)

The line-shape function developed by Levine and Birnbaum[23] and modified by Hunt and Poll[24] was used. The normalized spectral function is defined by

$$F(\Delta\nu,\delta)=a\left[1+\exp\left[-\frac{hc\Delta\nu}{kT}\right]\right]^{-1}\left[\frac{q\Delta\nu}{\delta}\right]^2 \times K_2(q\Delta\nu/\delta)\ . \quad (7)$$

Here $\Delta\nu=\nu-\nu_0$, where ν_0 is the line center in wave numbers, δ is the line "half-width" at half maximum, $q=2.027$, K_2 is a modified Bessel function of the second kind, and a is a constant such that the integral of F over wave number is unity. The line absorption coefficient is then given by

$$\alpha(\nu)=\alpha(T)\nu F(\Delta\nu,\delta)\ \text{cm}^{-1}\,\text{amagat}^{-2} \quad (8)$$

where $\alpha(T)$ is the integrated absorption coefficient of a given transition. The total band strength is the sum of all such transitions. The linewidth is assumed to scale as

$$\delta=A\,(T/300)^{1/2} \quad (9)$$

where A is taken from room-temperature data but may be treated as a parameter. The computer code also allows for convolution of the spectrum with an instrumental slit function for comparison with the data. Note, however, that at the elevated temperatures of interest, the linewidths exceed the experimental resolution.

IV. DATA ANALYSIS AND INTERPRETATION

A. Argon

Most of the CIE data were taken with argon as a collision partner.[4] Measurements were typically performed for 20 mol% H_2–80 mol% Ar mixtures over the reflected shock temperature range of 900–2900 K. Selected measurements were also provided for other H_2 mixing ratios between 10% and 50%. The calibrated signal given in W/cm^2 sr μm was converted into spectral emissivity by taking the ratio of the signals to that expected of a blackbody at the same temperature. The spectral emissivities $\epsilon(\nu)$ which are proportional to the absorption coefficients $\alpha(\nu)$ are the basic results of the measurements. Typical data for argon mixtures are shown in Figs. 3 and 4. The lower traces shown in Figs. 3 and 4 correspond to emission observed behind shocks in pure argon performed under similar conditions. Continuous background radiation was always reproducibly observed in the argon shots. In interpreting the CIE emission observations, we took into account the fact that a background source contributed to the observed radiation, although the origin of this background was not identified. Note that the signal was well above background levels observed in pure Ar.

It is clear from the observed spectral band shape that the radiation is primarily Q branch, suggesting the domi-

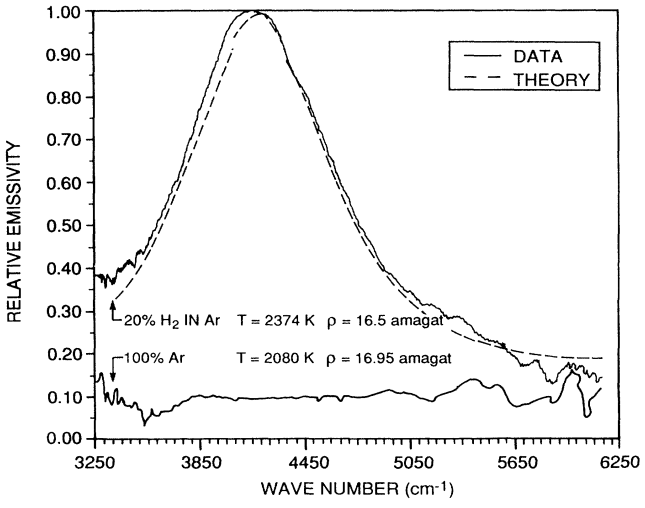

FIG. 3. Relative emissivity of the fundamental CIE vibration-rotation band of H_2 compared with typical background measurement in pure argon. Conditions as shown. --, synthetic spectrum of H_2 CIE band.

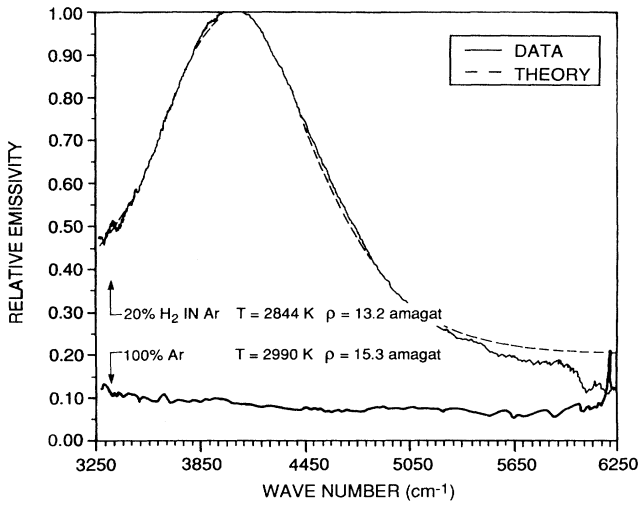

FIG. 4. Relative emissivity of the fundamental CIE vibration-rotation band of H_2 compared with a typical background measurement in pure argon. Conditions as shown. --, synthetic spectrum of H_2 CIE band.

nance of overlap induction at these temperatures (an S-branch feature would appear at ~ 5200 cm^{-1} if present). Computed spectral band shapes, using band strength parameters described below, were obtained using the analysis described in Sec. III and are shown in comparison with the data in Figs. 3 and 4. No evidence of the intercollisional interference dip[10] was observed in the data. Note that the average level of the background radiation (i.e., 100 mol % Ar) was added to the computed spectra. The agreement between theory and experiment is rather good, considering the approximate nature of the measurement and the various approximations in the calculations. Note that the linewidths used for this comparison were room-temperature values[25] of 160 and 110 cm^{-1} for the argon-induced overlap and quadrupolar transitions, respectively, scaled to the test temperatures from Eq. (9). The close comparison between measured and predicted band shapes, particularly in the band wings, clearly demonstrates the adequacy of this scaling law, as well as that of the various approximations in the calculations.

If there were no background radiation, the reduced mixture band strength could be deduced directly from the measured spectral emissivity through the relationship

$$\bar{\alpha}_M = (\bar{\nu} L \rho_M^2)^{-1} \int_0^\infty \epsilon(\nu) d\nu \tag{10}$$

where $\bar{\nu}$ is the band center frequency, 4160 cm^{-1}, L is the observation path length, 16.2 cm, and ρ_M is the gas density in amagats. The band strengths evaluated from Eq. (10) contain contributions due to both collision partners H_2 and Ar, namely,

$$\bar{\alpha}_M = [H_2](\alpha_{H_2,Ar}[Ar] + \alpha_{H_2,H_2}[H_2]) \tag{11}$$

where the brackets represent mole fraction. However, the second term was found to be negligible except for the H_2-Ne system.

A total of 12 H_2-Ar data sets were analyzed with Eq. (11) to provide evaluations of the H_2-Ar mixture reduced band strength over the temperature range 900–2900 K. The analysis was complicated by the presence of background radiation. Upper and lower limits of the band strength was determined by assuming that either all the observed emissivity was due to CIE, or that only the radiation above a line connecting the measured intensities at the highest and lowest wave numbers represents the CIE contribution. The results of this analysis are presented in Fig. 5 where the bars represent the upper and lower limits, and the symbols represent the best estimates of the measured band strength, obtained by subtracting the average background from the measured spectrum. (We have adopted these conservative bounds since we cannot rule out the possibility that the background radiation in the H_2-Ar mixtures is different than that observed in pure argon.)

The solid symbol shown in Fig. 5 corresponds to a measurement performed in a mixture of 10 mol % H_2–90 mol % Ar. In this case the observed band strength was scaled by a factor of 2 to allow comparison with the 20 mol % H_2 data. Similar measurements at the high temperatures performed in 50 mol % H_2–50 mol % Ar exhibited lower reduced band strengths than the 20 mol % H_2–80 mol % Ar data. These observations imply that H_2, at high temperatures, is a less efficient collision partner than Ar for producing H_2 CIE. These observations are supported by calculations which show that the H_2–rare-gas intensities are larger than the H_2-H_2 intensities, except for the case of H_2-Ne mixtures.

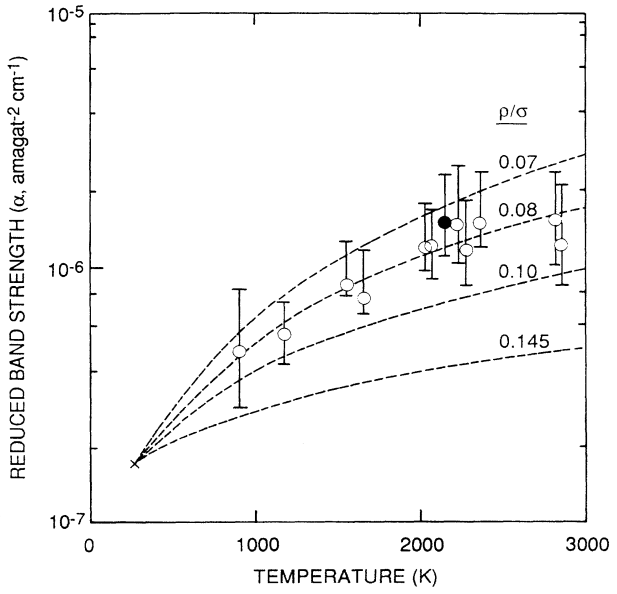

FIG. 5. Measured H_2 CIE fundamental vibration-rotation band strength vs temperature, specific to 20 mol % H_2–80 mol % Ar mixture. ●, scaled value for 10 mol % H_2–90 mol % Ar, × is from room-temperature absorption measurement.

The room-temperature value of α shown in Fig. 5 was scaled from earlier measurements[1] of the pure gas band strengths by use of Eq. (11). Note the almost order-of-magnitude increase in band strength between room temperature and 2900 K. This observed temperature dependence is much stronger than that expected for quadrupolar induction (almost independent of temperature, see, for example, Ref. 8) once again providing strong evidence that the high-temperature emission is dominated by overlap induction. The relative contribution of the overlap term was evaluated by use of known parameters for the quadrupolar contribution. The Lennard-Jones parameters used in the analysis are from Ref. 9 and listed in Table I. The values of $\bar{\gamma}\mu^2$ listed there were determined by means of a theoretical evaluation of the H_2 quadrupole moment.[26]

It was found in this work that 43% of the measured room-temperature H_2-Ar band strength[1] of 9.2×10^{-7} amagat^{-2}cm^{-1} is due to the quadrupole interaction $[(\mu_1^2+\mu_2^2)\tilde{J}\bar{\gamma}$, see Eq. (1)] and thus that the quantity $\lambda^2 I\bar{\gamma}$ for H_2-Ar is 5.3×10^{-7} amagat^{-2}cm^{-1} at room temperature. The data of Fig. 5 were analyzed under the assumption that Ar is the dominant (sole) collision partner. The theoretical predictions shown in Fig. 5 correspond to different pairs of ρ,ξ all chosen to provide the same H_2-Ar overlap contribution at room temperature. As can be seen, the value of the range parameter $\rho/\sigma=0.145$, which was originally suggested by Van Kranendonk,[9] and used by Linsky,[8] does not provide agreement with the observed temperature dependence of the data. A value $\rho/\sigma=0.08$ appears to be more appropriate. This analysis is approximate inasmuch as the observed radiation is due in some small part to the H_2 collision partner which was neglected, and because of the potential whose form was roughly approximated. This is the first evaluation of the reduced range of the overlap-induced moment, ρ/σ, from measurements at elevated temperatures. McTaggart and Welsh[20] performed a detailed analysis of the spectral shape of the H_2-Ar fundamental absorption band over the temperature range of 77–300 K. From an analysis of the intercollisional interference dip,[10] a phenomenon not observed in the present work, they estimated that $\rho/\sigma\sim0.08$, which is in good agreement with our results. Our value of ρ/σ is also in good agreement with the recent theoretical value of Meyer and Frommhold.[27]

B. Xenon

Only limited measurements were performed with xenon because of the high cost of filling the shock tube with this gas. Typical results for a 20 mol% H_2–80 mol% Xe mixture are shown in Figs. 6 and 7, along with computed band shapes. The data for H_2-Xe appear similar to the data shown earlier for Ar, except that the noise level seems higher. There may be some underlying S-band radiation at higher wave numbers inasmuch as the quadrupole contribution for xenon is approximately three times that for argon. Indeed the emission data of Fig. 6 exhibit some structure at ~5400 cm^{-1}, approximately where S-band contributions would peak. Unfortunately, no measurements were made in pure xenon to evaluate the true level of background emission. The limits of the measured band strengths for this mixture were deduced in a manner analogous to that for H_2-Ar and are displayed in Fig. 8. Shown for comparison is a calculation normalized to the observed room-temperature value of the band strength[1] and a value of ρ/σ of 0.14. As can be seen the theory predicts no prominent S-band feature for this choice of parameters. Although the agreement is quite reasonable, we believe that our data are too limited to constitute an independent determination of ρ/σ. Indeed, a value of ρ/σ of 0.12 has been reported for xenon in Ref. 21. Use of this value would only cause a $\sim20\%$ variation in the computed value of band strength, well within the uncertainty of the data.

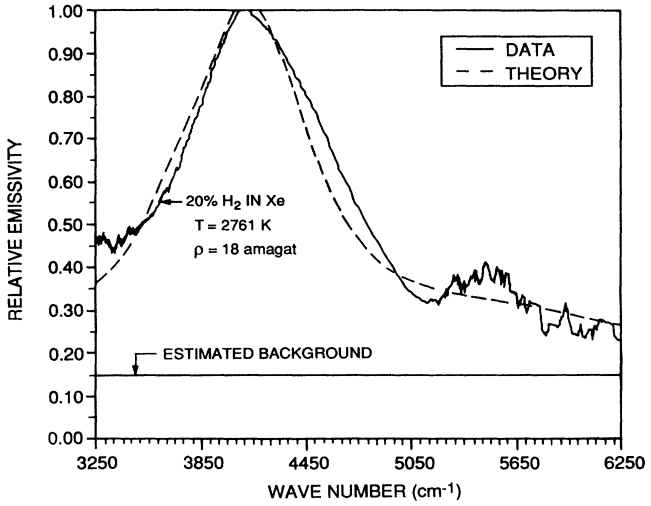

FIG. 6. Relative spectral emissivity for 20 mol% H_2–80 mol% Xe.

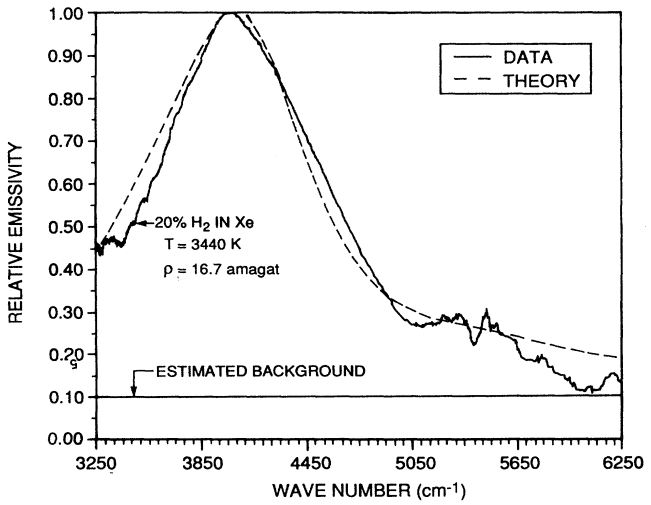

FIG. 7. Relative spectral emissivity for 20 mol% H_2–80 mol% Xe.

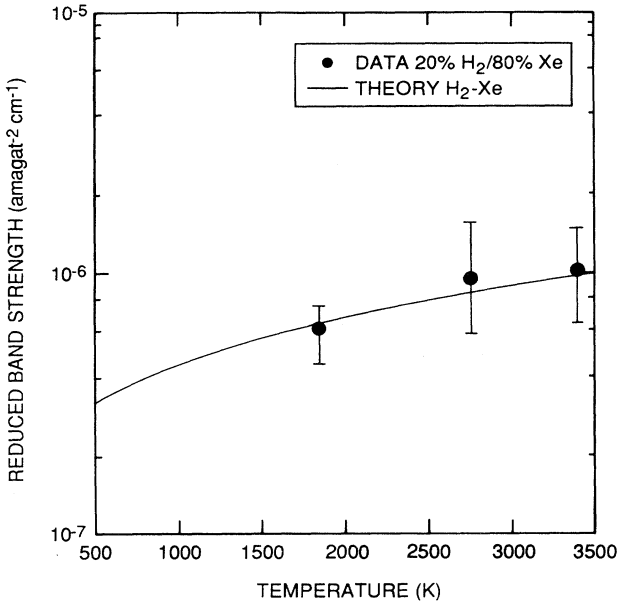

FIG. 8. Comparison between measured and predicted band strength for H_2 fundamental band 20 mol % H_2–80 mol % Xe.

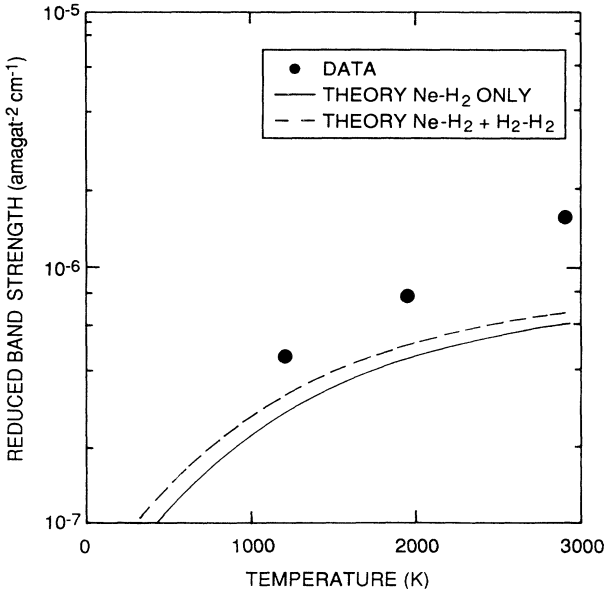

FIG. 10. Comparison between measured and predicted reduced band strength for H_2 fundamental band 20 mol % H_2–80 mol % Ne. The data are strong upper bounds.

C. Neon

Neon was the least efficient collision partner. Radiation levels were quite low, and the ratio of signal to noise was ~2. A typical result is shown in Fig. 9. Although the CIE band is clearly present, the signal fluctuations are quite large. The relative noise level was found to increase with increasing temperature. Data such as these could only be used to provide a strong upper bound for the band strength by assuming that all the observed emission in the spectral region of the band was due to CIE.

The resulting upper limits for the band strengths are shown in Fig. 10. These are compared with a calculation for neon made by utilizing the overlap dipole parameters listed in Table I, which were evaluated by Reddy and Chang[21] from low-temperature (< 300 K) data. Since neon is the least efficient of the collision partners considered, the possible contribution of H_2-H_2 collisions to

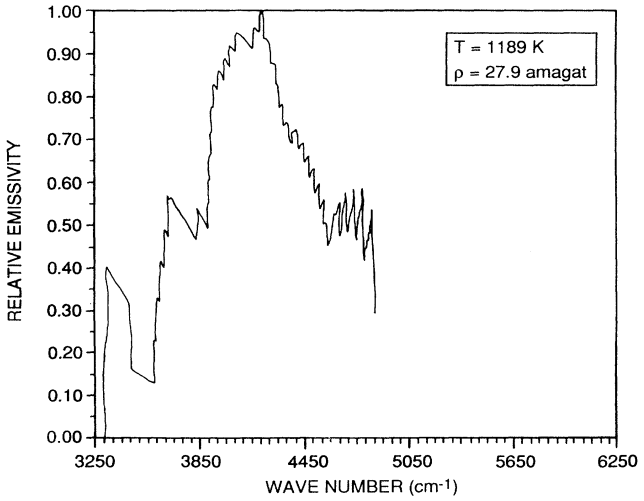

FIG. 9. Relative spectral emissivity for 20 mol % H_2–80 mol % Ne.

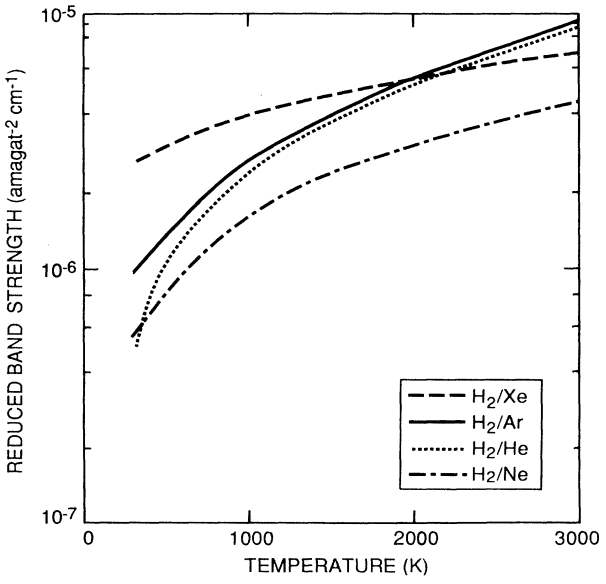

FIG. 11. Theoretical predictions for reduced band strength for H_2–rare-gas collisions for the H_2 fundamental band using Eq. (1).

the total observed band strengths was also estimated using H_2 parameters from Ref. 9. This contribution is shown as the dashed line in the figure, and it can be seen that the H_2-H_2 contribution is indeed modest. The computed curves are below the observed upper bounds and follow a similar temperature dependence. Nevertheless, we can state that predictions made using a low-temperature evaluation of the overlap dipole parameters are consistent with our high-temperature data.

D. Helium

Helium is a particularly important CIE collision partner for stellar atmospheres. Unfortunately, light gases such as He are not readily amenable to conventional shock heating; thus no measurements were performed. The temperature-dependent band strength for He was evaluated, however, using the overlap dipole parameters of Reddy and Chang,[21] and these results are presented with H_2-Ne, H_2-Ar, and He-Xe in Fig. 11. The only other published high-temperature CIE band strength predictions for He are those of Linsky.[8] These earlier predictions utilized a higher value of ρ/σ than presently used and consequently fall a factor of 5 below the values presented in Fig. 11 at high temperature. This large difference clearly demonstrates the importance of an accurate overlap-induced dipole for higher-temperature applications.

V. SUMMARY

The first observations of collision-induced emission in the fundamental vibration-rotation band of hydrogen have been presented for Ar, Xe, and Ne collision partners. At temperatures between 1000 and 3400 K, we found that the CIE emission was primarily from Q-band transitions involving the overlap-induced dipoles. These high-temperature measurements allow probing of the induced dipole at closer interaction distances than have been accessible through lower-temperature absorption measurements. We interpreted the measurements in terms of the theory of Van Kranendonk,[9] which, despite uncertainties in the data and potential function and approximations in the analysis, adequately represents the data over this temperature range. Indeed, in the case of argon and xenon, dipole interaction parameters evaluated from absorption data taken at temperatures at 300 K and below were found to be valid at the high temperatures of the present measurements.

ACKNOWLEDGMENTS

This research was supported by the National Science Foundation under Grant No. CPE-8212787 and was monitored by Dr. R. Rosenbach and Dr. E. Sparrow.

[1]H. L. Welsh, *International Reviews of Science, Physical Chemistry, Spectroscopy* (Butterworths, London, 1972), Vol. 3, Chap. 2, pp. 33–71.
[2]S. P. Reddy, in *Phenomena Induced by Intermolecular Interactions,* Vol. 127 of *NATO Advanced Study Institute, Series B: Physics,* edited by G. Birnbaum (Plenum, New York, 1985), pp. 129–167.
[3]R. Krech, G. Caledonia, S. Schertzer, K. Ritter, T. Wilkerson, L. Cotnoir, R. Taylor, and G. Birnbaum, Phys. Rev. Lett. **49**, 1913 (1982).
[4]G. E. Caledonia, R. H. Krech, T. Wilkerson, R. L. Taylor, and G. Birnbaum, in *Shock Waves and Shock Tubes,* edited by D. Bershader and R. Hanson (Stanford University Press, Stanford, 1986), pp. 835–841.
[5]D. Goorvitch and R. H. Tipping, J. Quant. Spectrosc. Radiat. Transfer **27**, 399 (1982).
[6]R. Hanel, B. Conrath, M. Flasar, V. Kunde, P. Lowman, W. Maguire, J. Pearl, J. Pirraglia, R. Samuelson, D. Gautier, P. Gierasch, S. Kumar, and C. Ponnamperuma, Science **204**, 972 (1979).
[7]V. Fine and H. Larson, Astrophys. J. **233**, 1021 (1979).
[8]J. L. Linsky, Astrophys. J. **156**, 989 (1969).
[9]J. Van Kranendonk, Physica (Utrecht) **23**, 825 (1957); J. Van Kranendonk and J. Z. Kiss, Can. J. Phys. **37**, 1187 (1959).
[10]J. Van Kranendonk, Can. J. Phys. **46**, 1173 (1968).
[11]J. C. Camm, R. L. Taylor, and R. Lynch, Appl. Opt. **6**, 885 (1967).
[12]R. H. Krech and G. E. Caledonia, J. Eng. Comput. Appl. **1**, 25 (1987).
[13]G. E. Caledonia, R. H. Krech, and T. Wilkerson, J. Quant. Spectrosc. Radiat. Transfer **34**, 183 (1985).
[14]C. Chackerian, Jr. and R. H. Tipping, J. Mol. Spectrosc. **99**, 431 (1984); C. Chackerian, Jr. (private communication).
[15]E. F. Green and J. P. Toennies, *Chemical Reaction in Shock Waves* (Arnold, London, 1964).
[16]R. J. LeRoy and J. Van Kranendonk, J. Chem. Phys. **61**, 4750 (1974).
[17]R. J. LeRoy and J. M. Hutson, J. Chem. Phys. **86**, 837 (1987).
[18]L. Frommhold and W. Meyer, Phys. Rev. A **35**, 632 (1987).
[19]J. O. Hirschfelder, C. F. Curtis, and R. B. Bird, *Molecular Theory of Gasses and Liquids* (Wiley, New York, 1954).
[20]J. W. McTaggart and H. L. Welsh, Can. J. Phys. **51**, 158 (1973).
[21]S. P. Reddy and K. S. Chang, J. Mol. Spectrosc. **47**, 22 (1973).
[22]J. L. Hunt and J. D. Poll, Can. J. Phys. **56**, 950 (1978).
[23]H. B. Levine and G. Birnbaum, Phys. Rev. **154**, 86 (1976).
[24]J. L. Hunt and J. D. Poll, J. Phys. **56**, 950 (1978).
[25]J. L. Hunt and H. L. Welsh, Can. J. Phys. **42**, 873 (1964).
[26]J. D. Poll and L. Wolniewicz, J. Chem. Phys. **68**, 3053 (1978).
[27]W. Meyer and L. Frommhold, Phys. Rev. A **14**, 2936 (1986).